Rapidly driven nanoparticles: mean first-passage times and relaxation of the magnetic moment

Stanislav I. Denisov, K. Sakmann, Peter Talkner, Peter Hänggi

Rapidly driven nanoparticles: Mean first-passage times and relaxation of the magnetic moment

S. I. Denisov,[1,2] K. Sakmann,[1] P. Talkner,[1] and P. Hänggi[1]

[1]*Institut für Physik, Universität Augsburg, Universitätsstraße 1, D-86135 Augsburg, Germany*
[2]*Sumy State University, 2 Rimsky-Korsakov Street, 40007 Sumy, Ukraine*
(Received 31 January 2007; revised manuscript received 26 March 2007; published 24 May 2007)

We present an analytical method of calculating the mean first-passage times (MFPTs) for the magnetic moment of a uniaxial nanoparticle which is driven by a rapidly rotating, circularly polarized magnetic field and interacts with a heat bath. The method is based on the solution of the equation for the MFPT derived from the two-dimensional backward Fokker-Planck equation in the rotating frame. We solve these equations in the high-frequency limit and perform precise, numerical simulations which verify the analytical findings. The results are used for the description of the rates of escape from the metastable domains, which in turn determine the magnetic relaxation dynamics. A main finding is that the presence of a rotating field can cause a drastic decrease of the relaxation time and a strong magnetization of the nanoparticle system. The resulting stationary magnetization along the direction of the easy axis is compared with the mean magnetization following from the stationary solution of the Fokker-Planck equation.

I. INTRODUCTION

The problem of finding the statistical characteristics of the first, the biggest, and the like, for sample paths of a stochastic process, frequently occurs in physics, biology, economics, and other sciences.[1–3] A particularly prominent identifier is the mean first-passage time (MFPT), i.e., the average value of the random times taken by a random walker that starts out from some initial state to reach another prescribed state in state space for the first time. This quantity describes a large variety of noise-induced effects such as activation rates or reaction rates, the lifetime of metastable states, the extinction of populations, or the extreme events in financial time series, to name only a few. Unfortunately, the class of stochastic processes for which the MFPT can be calculated explicitly is rather restricted. In fact, the most general analytical results were obtained for one-dimensional discrete or continuous Markov processes that are homogeneous in time.[4–7] However, these conditions of one-dimensionality and time homogeneity often represent an oversimplification. In particular, Markov processes that describe time-dependent systems are usually not homogeneous. Prominent examples are Brownian motors and ratchetlike stochastic systems,[8,9] as well as systems exhibiting stochastic resonance.[10,11] Although a few advanced, approximate methods for the analysis of periodically driven Markovian systems are available,[12–19] the development of new approaches for calculating the MFPTs in such systems still presents an important challenge.

In this paper, we develop an analytical approach to the two-dimensional MFPT problem for a magnetic moment of a ferromagnetic nanoparticle driven by a magnetic field which rapidly rotates in the plane perpendicular to the easy axis of magnetization (up-down axis). The natural precession of the magnetic moment always occurs in the counterclockwise direction (when viewed from above). Therefore, its deterministic dynamics in the up and down states differ.[20] For this reason the stochastic dynamics and thus the MFPTs in these states are different as well. In turn, the difference in the MFPTs can drastically change the magnetic properties of

systems composed of nanoparticles. This was explicitly shown in the resonant case, when the driving frequency coincides with the Larmor frequency of precession.[21] With this work we present a detailed analysis of this phenomenon in the case of a rapidly rotating magnetic field, which was briefly presented in Ref. 22, and apply the MFPTs for describing the thermally activated magnetic relaxation in such systems.

The paper is structured as follows. In Sec. II, we present the model and introduce the stochastic Landau-Lifshitz equation together with the corresponding forward and backward Fokker-Planck equations in the rotating frame. In Sec. III, we derive the general two-dimensional equations that define the MFPTs for the driven magnetic moment of a uniaxial nanoparticle in the up and down states. The analytical solution of these equations in the case of a rapidly rotating magnetic field is carried out in Sec. IV. In the same section, to verify our method, we solve the effective stochastic Landau-Lifshitz equations and calculate the MFPTs numerically. Some applications of the obtained results are presented in Sec. V. Here we study the features of magnetic relaxation and steady-state magnetization induced by a rapidly rotating field in nanoparticle systems. We summarize and discuss our findings in Sec. VI.

II. MODEL AND BASIC EQUATIONS IN THE ROTATING FRAME

Let us consider a simple model of a uniaxial ferromagnetic nanoparticle within which the nanoparticle is characterized only by the anisotropy field H_a and the magnetic moment $\mathbf{m}(t)$ of fixed length $|\mathbf{m}(t)| = m$. This model is relevant for nanoparticles whose sizes do not exceed the exchange length, i.e., the length scale below which the exchange interaction is predominant. We assume also that perpendicular to the easy axis of magnetization, which we choose as the z axis of a Cartesian coordinate system xyz, a circularly polarized magnetic field $\mathbf{h}(t) = h(\cos \omega t, \rho \sin \omega t, 0)$ is applied. Here, $h = |\mathbf{h}(t)|$ is the field amplitude, ω is the angular field fre-

quency, and $\rho=-1$ or $+1$ for clockwise and counterclockwise rotation of $\mathbf{h}(t)$, respectively.

We take into account the influence of a heat bath by means of damping and the presence of a thermal, Gaussian-distributed magnetic field $\mathbf{n}(t)$, possessing zero mean and the white noise correlations $\langle n_\alpha(t_1) n_\beta(t_2) \rangle = 2\Delta \delta_{\alpha\beta} \delta(t_2 - t_1)$. Here, $n_\alpha(t)$ $(\alpha, \beta = x, y, z)$ are the Cartesian components of $\mathbf{n}(t)$, Δ is the intensity of the thermal field, $\delta_{\alpha\beta}$ is the Kronecker symbol, $\delta(t)$ is the Dirac δ function, and the angular brackets denote averaging with respect to the sample paths of $\mathbf{n}(t)$. In this case the dynamics of $\mathbf{m}(t)$ is Markovian and can be described by the stochastic Landau-Lifshitz equation

$$\frac{d}{dt}\mathbf{m} = -\gamma \mathbf{m} \times (\mathbf{H}_{\text{eff}} + \mathbf{n}) - \frac{\lambda \gamma}{m} \mathbf{m} \times (\mathbf{m} \times \mathbf{H}_{\text{eff}}), \quad (2.1)$$

where $\gamma > 0$ denotes the gyromagnetic ratio, λ (>0) is the dimensionless damping parameter, $\mathbf{H}_{\text{eff}} = -\partial W / \partial \mathbf{m}$ is the effective magnetic field acting on $\mathbf{m}(t)$, W denotes the magnetic energy of a nanoparticle, and $\times$ indicates the vector product. The stochastic Landau-Lifshitz equation in the form of (2.1) was introduced by Kubo and Hashitsume.[23] Another form of this equation (with Gilbert's relaxation term[24]) was employed by Brown in his well-known paper.[25] We note, however, that although the solutions of these equations for a given realization of $\mathbf{n}(t)$ are generally different, their statistical characteristics are the same[26] (to within a renormalization factor for Δ). At present, both forms of the stochastic Landau-Lifshitz equation are used equally often. Although in the Langevin equation (2.1) the noise enters in a multiplicative manner, the resulting process actually is independent of the stochastic calculus if restricted to the sphere $\mathbf{m}^2(t) = m^2$. This is so because the corresponding, noise-induced drift terms are perpendicular to the sphere for any interpretation of the stochastic differential equation (2.1).[27–30] For the sake of definiteness, upon performing nonlinear transformations of this stochastic differential equation we shall consistently employ the Stratonovich interpretation.[31] We next perform such a nonlinear transformation by considering the dynamics of $\mathbf{m}(t)$ in terms of spherical coordinates in a rotating frame.

Specifically, using the respective polar and azimuthal angles θ and φ of the magnetic moment $\mathbf{m}(t) = m(\sin\theta\cos\varphi, \sin\theta\sin\varphi, \cos\theta)$, the magnetic energy W emerges as

$$W = \frac{1}{2}mH_a \sin^2\theta - mh\sin\theta\cos(\varphi - \rho\omega t). \quad (2.2)$$

The energy W depends on φ and t only through the single variable $\psi = \varphi - \rho\omega t$. Therefore, it is advantageous to introduce a rotating Cartesian coordinate system $x'y'z'$ (see also a similar description of a noisy, periodically driven Van der Pol oscillator in Ref. 32), in which $\mathbf{h}(t) = h(1, 0, 0)$ and the azimuthal angle φ is changed by ψ. According to Eq. (2.1), in this coordinate system the equations for θ and ψ can be written in the dimensionless form as follows:

$$\dot{\theta} = u(\theta, \psi) + \xi_\theta(\theta, \psi, \tau),$$

$$\dot{\psi} = v(\theta, \psi) - \rho\Omega + \xi_\psi(\theta, \psi, \tau). \quad (2.3)$$

Here, an overdot denotes the derivative with respect to the dimensionless time $\tau = \omega_r t$ with the Larmor frequency $\omega_r = \gamma H_a$, and $\Omega = \omega / \omega_r$ is the corresponding dimensionless frequency of the driving field. The functions $u(\theta, \psi)$ and $v(\theta, \psi)$ result as

$$u(\theta, \psi) = -\frac{1}{\sin\theta}\left(\lambda\sin\theta\frac{\partial}{\partial\theta} + \frac{\partial}{\partial\psi}\right)\widetilde{W},$$

$$v(\theta, \psi) = \frac{1}{\sin^2\theta}\left(\sin\theta\frac{\partial}{\partial\theta} - \lambda\frac{\partial}{\partial\psi}\right)\widetilde{W} \quad (2.4)$$

with $\widetilde{W} = W(\theta, \psi) / mH_a$ denoting the dimensionless magnetic energy. The stochastic forces $\xi_{\theta,\psi}(\theta, \psi, \tau)$ are determined as

$$\xi_\theta = -\widetilde{n}_{x'}(\tau)\sin\psi + \widetilde{n}_{y'}(\tau)\cos\psi,$$

$$\xi_\psi = \widetilde{n}_z(\tau) - [\widetilde{n}_{x'}(\tau)\cos\psi + \widetilde{n}_{y'}(\tau)\sin\psi]\cot\theta, \quad (2.5)$$

where $\widetilde{n}_{x'}(\tau) = \widetilde{n}_x(\tau)\cos\Omega\tau + \rho\widetilde{n}_y(\tau)\sin\Omega\tau$, $\widetilde{n}_{y'}(\tau) = \widetilde{n}_y(\tau)\cos\Omega\tau - \rho\widetilde{n}_x(\tau)\sin\Omega\tau$, and $\widetilde{n}_\alpha(\tau) = n_\alpha(\tau/\omega_r)/H_a$ are the components of the reduced thermal magnetic field. Using the statistical characteristics of $n_\alpha(t)$, for these components we readily obtain $\langle \widetilde{n}_\alpha(\tau) \rangle = 0$ and $\langle \widetilde{n}_\alpha(\tau_1)\widetilde{n}_\beta(\tau_2) \rangle = 2\widetilde{\Delta}\delta_{\alpha\beta}\delta(\tau_2 - \tau_1)$. Here, $\widetilde{\Delta} = \Delta\gamma/H_a$ is the dimensionless intensity of the reduced thermal field. With the help of the Sutherland-Einstein relation,[33] i.e., $\Delta = \lambda k_B T / \gamma m$ wherein k_B denotes the Boltzmann constant and T is the absolute temperature, it can be written also in the form $\widetilde{\Delta} = \lambda/2a$, where

$$a = mH_a/2k_BT \quad (2.6)$$

is the anisotropy barrier height in the units of the thermal energy $k_B T$. We note that, in the purely deterministic case, when $\widetilde{\Delta} = 0$, some important features of the solution of Eqs. (2.3) were studied in the context of the nonlinear dynamics of $\mathbf{m}(t)$ and its stability.[20,36]

Next we introduce the conditional probability density $P = P(\theta, \psi, \tau | \theta', \psi', \tau')$ $(\tau \geq \tau')$ which presents the most important statistical characteristic of the solution of Eqs. (2.3). Using the well-known connection between a set of stochastic differential equations and the corresponding Fokker-Planck equation (see, e.g., Refs. 2, 6, 28, and 37), we obtain the two-dimensional forward Fokker-Planck equation

$$\frac{\lambda}{2a}\left(\frac{\partial^2 P}{\partial\theta^2} + \frac{1}{\sin^2\theta}\frac{\partial^2 P}{\partial\psi^2}\right) - \frac{\partial}{\partial\theta}\left(\frac{\lambda}{2a}\cot\theta + u(\theta, \psi)\right)P$$

$$- \frac{\partial}{\partial\psi}[v(\theta, \psi) - \rho\Omega]P = \frac{\partial P}{\partial\tau} \quad (2.7)$$

and the corresponding backward Fokker-Planck equation

$$\frac{\lambda}{2a}\left(\frac{\partial^2 P}{\partial\theta'^2}+\frac{1}{\sin^2\theta'}\frac{\partial^2 P}{\partial\psi'^2}\right)+\left(\frac{\lambda}{2a}\cot\theta'+u(\theta',\psi')\right)\frac{\partial P}{\partial\theta'}$$

$$+[v(\theta',\psi')-\rho\Omega]\frac{\partial P}{\partial\psi'}=-\frac{\partial P}{\partial\tau'}. \qquad (2.8)$$

Notably, this two-dimensional Fokker-Planck dynamics does not obey a detailed balance symmetry,[28,37] if the driving frequency Ω does not vanish. In the model under consideration we have $\widetilde{W}=(1/2)\sin^2\theta-\widetilde{h}\sin\theta\cos\psi$, where $\widetilde{h}=h/H_a$. Therefore

$$u(\theta,\psi)=-\lambda\sin\theta\cos\theta+\widetilde{h}(\lambda\cos\theta\cos\psi-\sin\psi),$$

$$v(\theta,\psi)=\cos\theta-\widetilde{h}\frac{\cos\theta\cos\psi+\lambda\sin\psi}{\sin\theta}. \qquad (2.9)$$

The probability density P must satisfy the equal-time condition $P|_{\tau=\tau'}=\delta(\theta-\theta')\delta(\psi-\psi')$ and appropriate boundary conditions, as implied by the physical context. Moreover, in spite of the singularities in Eqs. (2.7) and (2.8) at $\theta,\theta'=0,\pi$ (which are a consequence of the use of the spherical coordinate system), the probability density P must be a regular function also at these points. In addition, if not excluded by the boundary conditions, P must be properly normalized, i.e., $\int_0^{2\pi}d\psi\int_0^{\pi}d\theta\, P=1$. We note also that the forward and backward Fokker-Planck equations (2.7) and (2.8) are equivalent; the difference between them is which set of variables, θ,ψ,τ or θ',ψ',τ', is held fixed. Due to this difference, the former is more convenient for studying the statistical properties of the magnetic moment $\mathbf{m}(t)$ as a function of the evolving time t, while the latter is more appropriate in studying the first-passage time statistics for $\mathbf{m}(t)$.

Based on the Fokker-Planck equation (2.7) one can determine stochastically equivalent Langevin equations, reading

$$\dot{\theta}=u(\theta,\psi)+\frac{\lambda}{2a}\cot\theta+\sqrt{\frac{\lambda}{a}}\eta_\theta(\tau),$$

$$\dot{\psi}=v(\theta,\psi)-\rho\Omega-\sqrt{\frac{\lambda}{a}}\frac{1}{\sin\theta}\eta_\psi(\tau), \qquad (2.10)$$

where $\eta_\theta(\tau)$ and $\eta_\psi(\tau)$ denote two independent Gaussian white noise sources with zero mean and white noise correlations $\langle\eta_i(\tau)\eta_j(\tau')\rangle=\delta_{ij}\delta(\tau-\tau')$, wherein $i,j=\theta,\psi$. In spite of the multiplicative nature involving the noise $\eta_\psi(\tau)$ in the second equation, the resulting stochastic dynamics possesses a vanishing noise-induced drift and thus is again independent of the employed stochastic calculus.[29,30] As a basis for numerical investigations the latter Langevin equations provide a more convenient starting point than Eqs. (2.3); this is so because they require the simulation of only two, rather than three, independent Gaussian white noises.

III. GENERAL EQUATIONS FOR THE MFPTs

In the absence of the random magnetic field, i.e., for $\mathbf{n}(t)=\mathbf{0}$, or equivalently $\Delta=0$, the motion of the magnetic moment follows the deterministic Landau-Lifshitz equations. In the rotating frame, the resulting deterministic dynamical system is not explicitly dependent on time and is given in terms of two degrees of freedom. For $\lambda>0$ this constitutes a dissipative system, which can only perform regular motion approaching fixed points or limit cycles in the asymptotic limit of large times. In the present paper, we are mainly interested in values of the parameters λ, $\widetilde{h}$, and Ω for which the motion is bistable, i.e., the asymptotic motion does lead to either of two attractors depending on the initial condition. These attractors are denoted as up and down states and labeled by $\sigma=+1$ and -1, respectively. The dynamics generates a partition of the state space into two domains of attraction, each containing either the up or the down state. The common boundary between the domains of attraction is formed by the separatrix.

In the presence of a random magnetic field the separatrix is no longer an impenetrable border, and transitions between the two domains of attraction may occur. For small random fields, corresponding to large values of a, these transitions are rare and can be characterized by transition rates. It is now tempting to determine the rate between a state σ and the opposite state by the MFPT to the separatrix, $\mathcal{T}_{\sigma\text{sep}}$, i.e., by the statistical average of the stochastic first-passage times of trajectories that start at the attractor σ and reach the separatrix for the first time. In the asymptotic limit of vanishing noise a trajectory visiting the separatrix will go to either side with equal probability, and the rate is given by the inverse of twice the mean first-passage time. For finite noise the transitions from the separatrix to the two sides may differ from each other,[34] whereby the precise value of the resulting bias in general is difficult to quantify.[35] In order to be more flexible, we consider the mean first-passage times to the boundaries of two regions $R_{+1}=\{\theta,\psi|0\leq\theta\leq\phi_{+1}(\psi),0\leq\psi<2\pi\}$ and $R_{-1}=\{\theta,\psi|\phi_{-1}(\psi)\leq\theta\leq\pi,0\leq\psi<2\pi\}$, each containing one attractor. The boundaries $\phi_\sigma(\psi)$ can be chosen as the separatrix or as any other curve between the two attractors. For a convenient choice of the boundaries $\phi_\sigma(\psi)$ we refer the reader to the next section. We note that the regions R_σ are stationary in the rotating frame but may move in the rest frame.

In order to determine the first-passage times of the regions R_σ, recrossings of the respective boundaries $\partial R_\sigma=\{\theta,\psi|\theta=\phi_\sigma(\psi),0\leq\psi\leq2\pi\}$ must be suppressed.[1] This is conveniently achieved by imposing absorbing boundary conditions on the conditional probability density $P_\sigma(\theta,\psi,\tau-\tau'|\theta',\psi')$ obeying the backward Fokker-Planck equation (2.8), i.e., we require $P_\sigma(\theta,\psi,\tau-\tau'|\theta',\psi')=0$ for $(\theta',\psi')\in\partial R_\sigma$. Here, we used the fact that in the rotating frame the process in the stationary regions R_σ is time homogeneous, with

$$P_\sigma(\theta,\psi,\tau-\tau'|\theta',\psi')\equiv P_\sigma(\theta,\psi,\tau-\tau'|\theta',\psi',0)$$

$$=P_\sigma(\theta,\psi,\tau|\theta',\psi',\tau'). \qquad (3.1)$$

If the magnetic moment starts out at the time τ' at the position $(\theta',\psi')\in R_\sigma$, it will uninterruptedly stay within the initial region R_σ until a time τ with a probability $Q(\theta',\psi';\tau-\tau')$. This probability can be expressed as the in-

tegral of the conditional probability density over all states in R_σ, i.e.,

$$Q_\sigma(\theta', \psi'; \tau - \tau') = \int_{R_\sigma} d\psi\, d\theta\, P_\sigma(\theta, \psi, \tau - \tau' | \theta' \psi').$$

$$(3.2)$$

The probability $Q_\sigma(\theta', \psi'; \tau - \tau')$ is a solution of the backward equation with the absorbing boundary conditions $Q_\sigma(\theta', \psi'; \tau - \tau') = 0$ for $(\theta', \psi') \in \partial R_\sigma$ and the initial condition $Q_\sigma(\theta', \psi'; 0) = 1$. Integrating $Q_\sigma(\theta', \psi'; \tau - \tau')$ over all positive (dimensionless) times $u \equiv \tau - \tau'$, one obtains an expression for the (dimensionless) MFPT of the form

$$T_\sigma(\theta', \psi') = \int_0^\infty du\, Q_\sigma(\theta', \psi'; u).$$

$$(3.3)$$

This MFPT is the solution of the backward equation

$$\frac{\lambda}{2a}\left(\frac{\partial^2 T_\sigma}{\partial\theta'^2} + \frac{1}{\sin^2\theta'}\frac{\partial^2 T_\sigma}{\partial\psi'^2}\right) + \left(\frac{\lambda}{2a}\cot\theta' + u(\theta',\psi')\right)\frac{\partial T_\sigma}{\partial\theta'}$$

$$+ [v(\theta',\psi') - \rho\Omega]\frac{\partial T_\sigma}{\partial\psi'} = -1 \qquad (3.4)$$

with the absorbing boundary conditions

$$T_\sigma(\theta', \psi') = 0 \quad \text{for } (\theta', \psi') \in \partial R_\sigma. \qquad (3.5)$$

Equation (3.4) was derived in Ref. 38 for the undriven case with $\Omega = 0$.

Because $u(\theta', \psi')$, $v(\theta', \psi')$, and also $T_\sigma(\theta', \psi')$ are periodic functions of ψ', it is convenient to decompose these functions into their average and periodically varying parts in ψ': $u(\theta', \psi') = \bar{u}(\theta') + u_1(\theta', \psi')$, $v(\theta', \psi') = \bar{v}(\theta') + v_1(\theta', \psi')$, and $T_\sigma(\theta', \psi') = \bar{T}_\sigma(\theta') + S_\sigma(\theta', \psi')$. Here, $\bar{u}_1(\theta', \psi') = \bar{v}_1(\theta', \psi') = \bar{S}_\sigma(\theta', \psi') = 0$, the overbar denotes an average over ψ', i.e., $\overline{(\cdot)} = (1/2\pi)\int_0^{2\pi} d\psi'(\cdot)$ and, according to (2.9),

$$\bar{u}(\theta') = -\lambda\sin\theta'\cos\theta', \quad \bar{v}(\theta') = \cos\theta',$$

$$u_1(\theta', \psi') = \tilde{h}(\lambda\cos\theta'\cos\psi' - \sin\psi'),$$

$$v_1(\theta', \psi') = -\tilde{h}\frac{\cos\theta'\cos\psi' + \lambda\sin\psi'}{\sin\theta'}. \qquad (3.6)$$

Using these decompositions, we find from Eq. (3.4) coupled equations (see also in Ref. 22) for the average part

$$\frac{\lambda}{2a}\left(\frac{d^2\bar{T}_\sigma}{d\theta'^2} + \cot\theta'\frac{d\bar{T}_\sigma}{d\theta'}\right) + \bar{u}\frac{d\bar{T}_\sigma}{d\theta'} + \overline{u_1\frac{\partial S_\sigma}{\partial\theta'}} + \overline{v_1\frac{\partial S_\sigma}{\partial\psi'}} = -1$$

$$(3.7)$$

and for the periodic part

$$\frac{\lambda}{2a}\left(\frac{\partial^2 S_\sigma}{\partial\theta'^2} + \frac{1}{\sin^2\theta'}\frac{\partial^2 S_\sigma}{\partial\psi'^2} + \cot\theta'\frac{\partial S_\sigma}{\partial\theta'}\right) + u_1\frac{d\bar{T}_\sigma}{d\theta'} + u\frac{\partial S_\sigma}{\partial\theta'}$$

$$+ (v - \rho\Omega)\frac{\partial S_\sigma}{\partial\psi'} - \overline{u_1\frac{\partial S_\sigma}{\partial\theta'}} - \overline{v_1\frac{\partial S_\sigma}{\partial\psi'}} = 0. \qquad (3.8)$$

We emphasize that these equations are fully exact, i.e., they follow from the stationary backward Fokker-Planck equation being in the rotating frame.

IV. RAPIDLY ROTATING FIELD

A. Analytical analysis for the MFPT

In the case of a rapidly rotating magnetic field, i.e., when the condition $\tilde{h}/\Omega \ll 1$ holds (note that $\tilde{h}$ need not be small), Eq. (3.8) can be essentially simplified.[22] The reason is that the function S_σ and its derivatives tend to zero as $\tilde{h}/\Omega \to 0$. Using these conditions and taking into account that for large frequencies the term $\Omega\partial S_\sigma/\partial\psi'$ is of the order Ω^0, we obtain from Eq. (3.8) the approximation

$$\rho\Omega\frac{\partial S_\sigma}{\partial\psi'} - u_1\frac{d\bar{T}_\sigma}{d\theta'} = 0. \qquad (4.1)$$

According to (3.6), the solution of Eq. (4.1) that satisfies the condition $\bar{S}_\sigma = 0$ is given by

$$S_\sigma = \rho\frac{\tilde{h}}{\Omega}(\lambda\cos\theta'\sin\psi' + \cos\psi')\frac{d\bar{T}_\sigma}{d\theta'}. \qquad (4.2)$$

This solution self-consistently conforms with the assumptions made above. Using Eqs. (4.2) and (3.6), we find

$$\overline{u_1\frac{\partial S_\sigma}{\partial\theta'}} = \overline{v_1\frac{\partial S_\sigma}{\partial\psi'}} = -\frac{\lambda}{2}\tilde{h}_{\text{eff}}\sin\theta'\frac{d\bar{T}_\sigma}{d\theta'}, \qquad (4.3)$$

where

$$\tilde{h}_{\text{eff}} = -\rho\tilde{h}^2/\Omega. \qquad (4.4)$$

With these results, Eq. (3.7) reduces to the form

$$\frac{\lambda}{2a}\frac{d^2\bar{T}_\sigma}{d\theta'^2} + \left(\frac{\lambda}{2a}\cot\theta' - \lambda(\cos\theta' + \tilde{h}_{\text{eff}})\sin\theta'\right)\frac{d\bar{T}_\sigma}{d\theta'} = -1.$$

$$(4.5)$$

According to this equation, a magnetic field rapidly rotating in the plane perpendicular to the easy axis of the nanoparticle acts on the nanoparticle's magnetic moment precisely as a static effective magnetic field $\tilde{h}_{\text{eff}}$ (in units of the anisotropy field H_a) which is applied along the easy axis. The direction of this field and the direction of the field rotation follow the left-hand rule and its value can be large enough to produce observable effects. Next we assume that $|\tilde{h}_{\text{eff}}| < 1$; otherwise, only one state, $\sigma = +1$ or $\sigma = -1$, is stable.

It is not difficult to show that the general solution of Eq. (4.5) contains both regular and singular parts.[39] The singular

part arises solely from the use of a spherical coordinate system and has no physical meaning. It exhibits a logarithmic singularity at $\theta' = \pi(1-\sigma)/2$ and, as a consequence, its derivative diverges. On the contrary, the regular part has a vanishing derivative at this point. Therefore, in order to exclude the contribution of the singular part, the solution of Eq. (4.5) must satisfy the regularity condition $(d\overline{\mathcal{T}}_\sigma/d\theta')|_{\theta'=\pi(1-\sigma)/2}=0$. We note in this context that the regularity condition corresponds to the situation when a reflecting barrier is placed at the point $\theta' = \pi(1-\sigma)/2$.

In order that the high-frequency approximation for the MFPTs can consistently be performed, the ψ dependence of the boundary curves $\phi_\sigma(\psi)$ must be chosen conveniently. Assuming that $\phi_\sigma(\psi') = \bar{\phi}_\sigma + \phi_{1\sigma}(\psi')$ with $\bar{\phi}_{1\sigma}(\psi')=0$ and $\phi_{1\sigma}(\psi') \sim \tilde{h}/\Omega$, the absorbing boundary condition (3.5) in the linear approximation in $\tilde{h}/\Omega$ leads to the relations $\overline{\mathcal{T}}_\sigma(\bar{\phi}_\sigma)=0$ and $\phi_{1\sigma}(\psi')(d\overline{\mathcal{T}}_\sigma/d\theta')|_{\theta'=\bar{\phi}_\sigma} + \mathcal{S}_\sigma(\bar{\phi}_\sigma, \psi')=0$. Using (4.2) and the latter relation, we find for the absorbing boundary the explicit form

$$\phi_\sigma(\psi) = \bar{\phi}_\sigma - \rho\frac{\tilde{h}}{\Omega}(\lambda \cos \bar{\phi}_\sigma \sin \psi + \cos \psi). \quad (4.6)$$

Next, solving Eq. (4.5) with the specified regularity and boundary conditions $(d\overline{\mathcal{T}}_\sigma/d\theta')|_{\theta'=\pi(1-\sigma)/2}=0$ and $\overline{\mathcal{T}}_\sigma(\bar{\phi}_\sigma)=0$, we obtain

$$\overline{\mathcal{T}}_\sigma(\theta') = \frac{2a}{\lambda} \int_{\cos \bar{\phi}_\sigma}^{\cos \theta'} dx \frac{e^{-a(x + \tilde{h}_{\mathrm{eff}})^2}}{1 - x^2} \int_x^\sigma dy \, e^{a(y + \tilde{h}_{\mathrm{eff}})^2}, \quad (4.7)$$

where $\theta' \in [0, \bar{\phi}_{+1}]$ if $\sigma=+1$, and $\theta' \in [\bar{\phi}_{-1}, \pi]$ if $\sigma=-1$. The angles $\bar{\phi}_\sigma$ can be chosen depending on the physical situation. For high potential barriers, i.e., $a \gg 1$, the magnetic moment predominantly dwells in the vicinity of either of two equilibrium states at $\theta=0$ and π. In this case, the transition times between the states σ and $-\sigma$ exceed by far the relaxation times toward these states. Therefore, in dimensional units the averaged MFPT $\bar{T}_\sigma(\theta') = \overline{\mathcal{T}}_\sigma(\theta')/\omega_r$ representing the transition time from one state σ to the opposite state $-\sigma$ only weakly depends on the precise location of the initial magnetization, as long as θ' lies within the domain of attraction of the considered state σ. Accordingly, the precise location of the absorbing boundary $\bar{\phi}_\sigma$ has practically no effect on $\bar{T}_\sigma(\theta')$ if it is located well beyond the separatrix which divides the state space into domains of attraction of up and down magnetization. Under these conditions, we find from (4.7) in leading order in a

$$\bar{T}_\sigma = \frac{\overline{\mathcal{T}}_\sigma}{\omega_r} = \frac{1}{\lambda\omega_r}\sqrt{\frac{\pi}{a}} \frac{\exp[a(1 + \sigma\tilde{h}_{\mathrm{eff}})^2]}{(1 - \tilde{h}_{\mathrm{eff}}^2)(1 + \sigma\tilde{h}_{\mathrm{eff}})}. \quad (4.8)$$

As follows upon inspection from (4.2) and (4.8), in the high-frequency limit the periodic part of $T_\sigma(\theta', \psi')$ can be neglected, i.e., $T_\sigma(\theta', \psi') \approx \bar{T}_\sigma$.

If $|\tilde{h}_{\mathrm{eff}}| \ll 1$ then (4.8) yields $\bar{T}_\sigma = T_0 \exp(\sigma 2a\tilde{h}_{\mathrm{eff}})$, where $T_0 = (1/\lambda\omega_r)\sqrt{\pi/a} \exp a$ is the MFPT at $\tilde{h}=0$. According to this formula, a rapidly rotating magnetic field increases the MFPT for the magnetic moment in the state $\sigma=-\rho$ ($\sigma\tilde{h}_{\mathrm{eff}} > 0$) and lowers this MFPT for the magnetic moment in the state $\sigma=+\rho$ ($\sigma\tilde{h}_{\mathrm{eff}} < 0$). This difference in the MFPTs arises from the natural precession of the nanoparticle magnetic moments, which occurs in the counterclockwise direction, if viewed from above. As a consequence, the statistical behavior of the up and down magnetic moments in the magnetic field rotating in a fixed direction is different.

Another choice of the position for the absorbing boundary can be made right on the separatrix itself. For the averaged one-dimensional dynamics of the azimuthal angle it corresponds to the θ value where the deterministic part of the drift of the reduced backward equation (4.5) assumes an unstable fixed point, i.e., for $\cos \theta = -\tilde{h}_{\mathrm{eff}}$, or, equivalently, to the maximum of the effective magnetic energy of the nanoparticle, $W_{\mathrm{eff}}(\theta) = mH_a[(1/2)\sin^2 \theta - \tilde{h}_{\mathrm{eff}} \cos \theta]$. Accordingly, the averaged dimensionless MFPT from an initial angle θ' to the separatrix reads

$$\overline{\mathcal{T}}_{\sigma \, \mathrm{sep}}(\theta') = \frac{2a}{\lambda} \int_{-\tilde{h}_{\mathrm{eff}}}^{\cos \theta'} dx \frac{e^{-a(x + \tilde{h}_{\mathrm{eff}})^2}}{1 - x^2} \int_x^\sigma dy \, e^{a(y + \tilde{h}_{\mathrm{eff}})^2}. \quad (4.9)$$

If $a \gg 1$ and $\cos \theta'$ is not too close to $-\tilde{h}_{\mathrm{eff}}$ then $\overline{\mathcal{T}}_{\sigma \, \mathrm{sep}}(\theta')$ only weakly depends on θ' and $\overline{\mathcal{T}}_{\sigma \, \mathrm{sep}} \to \overline{\mathcal{T}}_\sigma/2$ as $a \to \infty$. Thus, the ratio $\overline{\mathcal{T}}_{\sigma \, \mathrm{sep}}/\overline{\mathcal{T}}_\sigma$ between the MFPT to the separatrix and to an angle $\bar{\phi}_\sigma$ that is well beyond the separatrix converges to the value $1/2$ if $a \to \infty$; however, the larger the rotating field amplitude $\tilde{h}$ the slower is the convergence (see Fig. 1). We note also that for large but finite a the conditions $\overline{\mathcal{T}}_{\sigma \, \mathrm{sep}}/\overline{\mathcal{T}}_\sigma > 1/2$ and $\overline{\mathcal{T}}_{\sigma \, \mathrm{sep}}/\overline{\mathcal{T}}_\sigma < 1/2$ hold for $\sigma\rho=+1$ and $\sigma\rho=-1$, respectively. The reason is that the effective magnetic energy $W_{\mathrm{eff}}(\theta)$ has different slopes from the left and from the right of the separatrix disposed at $\theta=\arccos(-\tilde{h}_{\mathrm{eff}})$.

B. Numerical simulations

In order to examine the analytical results developed for calculating the MFPTs for a magnetic moment which is driven by a rapidly varying circularly polarized magnetic field, we performed numerical simulations of the full two-dimensional Langevin equations (2.10). For any given set of parameter values $\rho, \sigma, \Omega, a, \lambda, \tilde{h}$, four groups of 10^4 trajectories were run using a stochastic vector Euler algorithm.[2,40] All trajectories of a simulation were initialized with the same values for θ and ψ. In the vicinity of the coordinate singularity at $\theta=0$ a reflecting boundary was located at $\theta=0.02\pi$, together with an absorbing boundary at $\theta=0.8\pi$, which is located well beyond the separatrix of the corresponding deterministic system. The step width was chosen such that the increments in θ were less than $\pi/100$ and the increments in ψ less than $\pi/10$, respectively. The precise computation of
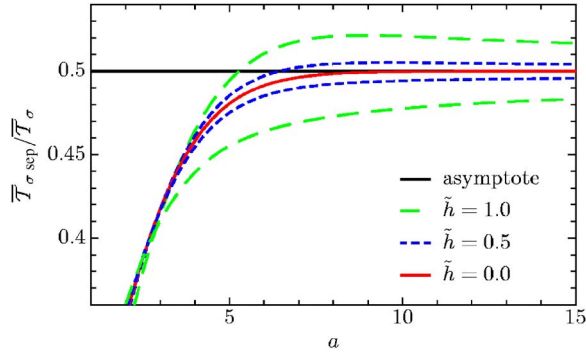
FIG. 1. (Color online) Dependence of the ratio $\bar{\mathcal{T}}_{\sigma\,\mathrm{sep}}/\bar{\mathcal{T}}_\sigma$ on the dimensionless anisotropy barrier height a for different values of the dimensionless amplitude $\tilde{h}$ of the rotating magnetic field. The numerical calculations of the integrals in the relations (4.7) and (4.9) were carried out for $\Omega = 10$, $\rho = +1$, $\bar{\phi}_{+1} = 0.9\pi$, $\bar{\phi}_{-1} = 0.1\pi$, $\theta' = 0.1\pi$ if $\sigma = +1$, and $\theta' = 0.9\pi$ if $\sigma = -1$. The broken curves (green and blue online) that cross the horizontal asymptote (black online) correspond to $\sigma = +1$, and the broken curves (green and blue online) that lie below the asymptote correspond to $\sigma = -1$. The solid curve (red online) represents the case $\tilde{h} = 0$ for which $\bar{\mathcal{T}}_{+1\,\mathrm{sep}}/\bar{\mathcal{T}}_{+1} = \bar{\mathcal{T}}_{-1\,\mathrm{sep}}/\bar{\mathcal{T}}_{-1}$. We note also that in all cases the ratio $\bar{\mathcal{T}}_{\sigma\,\mathrm{sep}}/\bar{\mathcal{T}}_\sigma$ does not depend on λ.

the MFPTs of this system using the Langevin equations (2.10) requires us to compute the arrival of all trajectories at the absorbing boundary. In practice, this method is unfeasible for all but the smallest values of the anisotropy barrier height a; this is so because a given trajectory can take much longer than the MFPT to arrive at the absorbing boundary. These events are rare, but contribute significantly to the MFPT, and hence a sufficiently large number of these events needs to be simulated to arrive at a reliable statistics. However, assuming that the first-passage time distribution is exponentially distributed with a rate parameter $1/\bar{T}_\sigma$ it is possible to determine the MFPT approximately by fitting the tail of the simulated first-passage time distribution to an exponential. Although this assumption can be justified for large barrier heights $a \gg 1$, since then the relaxation time of the system is much shorter than the MFPT, it clearly is expected to fail for $a \approx 1$. Note that a enters the exponent of the expression for the MFPT equation (4.7), and therefore the large barrier limit is already obtained for moderately large values of a. Using this assumption allows us to simulate the Langevin equations (2.10) for each trajectory up to a fixed maximal time at which on average a considerable fraction of all trajectories, but not all, have crossed the absorbing boundary. To be definite, we took this time to be two-thirds of the theoretical mean first-passage time calculated from Eq. (4.7). With this choice, roughly half of all trajectories arrived at the absorbing boundary. The number of absorbed transitions was stored as a function of time. From each of the resulting four data sets the rate $1/\bar{T}_\sigma$ was determined by an exponential fit and thereby the MFPT was estimated. From these four values an average value and a standard deviation was determined. The so obtained numerical findings compare most favorably with our theoretical predictions (see Figs. 2 and 3).
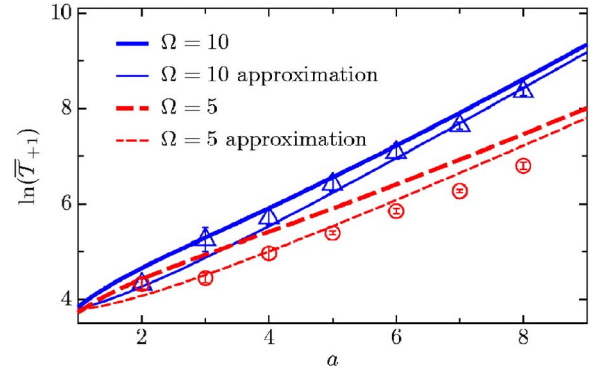

FIG. 2. (Color online) Natural logarithm of the dimensionless MFPT $\bar{\mathcal{T}}_{+1}$ as a function of the parameter a. The thick curves represent the exact theoretical results obtained from (4.7), and the thin curves depict the approximate high barrier limit given by (4.8). The symbols indicate results from the numerical simulation of 4×10^4 runs of the effective stochastic Landau-Lifshitz equations (2.10) with the initial conditions $\psi_0 = 0$, $\theta_0 = 0.05\pi$ and with the absorbing boundary at $\bar{\phi}_{+1} = 0.8\pi$. The broken curves and circular symbols (red online) correspond to $\Omega = 5$, and the solid curves and triangular symbols (blue online) correspond to $\Omega = 10$. In accordance with the theoretical assumption, the analytical results approach the numerical ones with increasing field frequency.

Figure 2 depicts the dependence of the MFPT as a function of the anisotropy barrier height a for two different driving angular frequencies $\Omega = 5$ and 10. The values of the other parameters are $\rho = +1$, $\sigma = +1$, $\tilde{h} = 1$, $\lambda = 0.1$. Depicted is the natural logarithm of the dimensionless MFPT $\bar{\mathcal{T}}_{+1}$. It can clearly be seen that the high-frequency predictions from Eqs. (4.7) and (4.8) approach the results of the numerical simulation from above as Ω is increased. This can be understood intuitively because the effective dynamic barrier for escape is
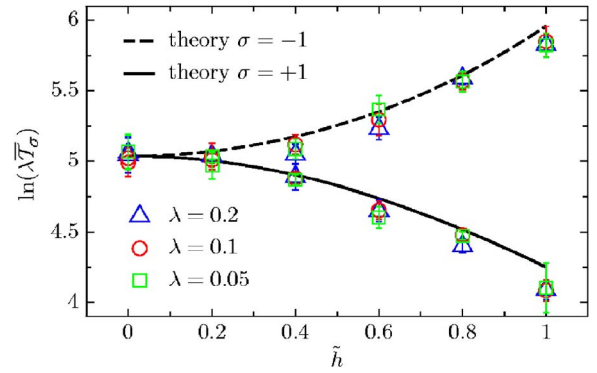

FIG. 3. (Color online) Natural logarithm of $\lambda\bar{\mathcal{T}}_\sigma$ as a function of the dimensionless amplitude $\tilde{h}$ of the rotating magnetic field. The solid and broken curves represent the theoretical results obtained from the relation (4.7) for $\sigma = +1$ and -1, respectively. The values of the other parameters are $a = 5$, $\Omega = 10$, and $\rho = +1$. The symbols (in color online) depict the results obtained from the numerical simulation of Eqs. (2.10) for different values of the damping parameter λ. In full agreement with theoretical predictions, $\ln(\lambda\bar{\mathcal{T}}_\sigma)$ as a function of $\tilde{h}$ decreases if $\sigma = +1$, increases if $\sigma = -1$, and does not depend on λ.

increased as Ω is increased. As expected, the agreement decreases in quality upon lowering the angular driving frequency; this fact is corroborated by the numerical results for $\Omega=5$ (the thick dashed line versus the numerical data points).

Figure 3 shows the dependence of the MFPT as a function of $\tilde{h}$, λ, and σ at constant $a=5$ and $\rho=+1$. As predicted by Eqs. (4.7) and (4.8), $\bar{T}_\sigma$ can be seen to be proportional to $1/\lambda$. The up and down states ($\sigma=+1$ and -1) are clearly inequivalent for nonzero $\tilde{h}$. This is in perfect agreement with the prediction of the theory, as can be deduced from the approximate equation (4.8) in which $\sigma=+1$ ($\sigma=-1$) decreases (increases) the exponent, since $\tilde{h}_{\text{eff}}<0$ for $\rho=+1$.

V. RELAXATION OF THE MAGNETIZATION

A. Relaxation law at high anisotropy barrier

The MFPTs $\bar{T}_\sigma$ provide important characteristics for the magnetic dynamics of nanoparticles. If their states σ are used for information storage then the average times during which the information in these states is kept safely must be considerably shorter than $\bar{T}_\sigma$. The dependence of $\bar{T}_\sigma$ on the characteristics of the rotating field gives the possibility to intentionally change the relative stability of the up and down states.

The transition times $\bar{T}_\sigma$ from the state σ to the state $-\sigma$ also determine the thermally activated magnetic relaxation in a system composed of uniaxial nanoparticles whose easy axes are perpendicular to the plane of field rotation. If $a \geq 1$ and the precession angle[20]

$$\theta_\sigma = \sqrt{\frac{1+\lambda^2}{(1-\sigma\rho\Omega)^2+\lambda^2}}\,\tilde{h} \qquad (5.1)$$

of the magnetic moment in the state σ is small, i.e., $\theta_\sigma^2 \ll 1$, the reduced magnetization of this system can be defined as $\mu(t)=[N_{+1}(t)-N_{-1}(t)]/N$, where $N_\sigma(t)$ denotes the number of nanoparticles in the state σ at time t, and N the whole number of particles. Taking into account that $N_{+1}(t)+N_{-1}(t)=N$, this definition yields $\dot{\mu}(t)=2\dot{N}_{+1}(t)/N$. Next, since the rate $1/\bar{T}_\sigma$ is the probability of reorientation of the magnetic moment from the state σ to the state $-\sigma$ per unit time, we have $\dot{N}_\sigma(t)=N_{-\sigma}(t)/\bar{T}_{-\sigma}-N_\sigma(t)/\bar{T}_\sigma$ and thus the equation for $\mu(t)$ takes the form

$$\dot{\mu}(t) = -\mu(t)\left(\frac{1}{\bar{T}_{+1}}+\frac{1}{\bar{T}_{-1}}\right)-\frac{1}{\bar{T}_{+1}}+\frac{1}{\bar{T}_{-1}}. \qquad (5.2)$$

Its solution with the initial condition $\mu(0)=1$ is given by

$$\mu(t) = (1-\mu_\infty)\exp(-t/t_{\text{rel}})+\mu_\infty, \qquad (5.3)$$

where $t_{\text{rel}}=\bar{T}_{+1}\bar{T}_{-1}/(\bar{T}_{+1}+\bar{T}_{-1})$ is the relaxation time and

$$\mu_\infty = \frac{\bar{T}_{+1}-\bar{T}_{-1}}{\bar{T}_{+1}+\bar{T}_{-1}} \qquad (5.4)$$

is the steady-state magnetization of the nanoparticle system induced by a rapidly rotating field.

A simple analysis shows that a rapidly rotating magnetic field causes a decrease of the relaxation time and magnetizes the nanoparticle system along the easy axis of magnetization ($t_{\text{rel}}<t_{\text{rel}}^{(0)}$ and $\mu_\infty \neq 0$ if $\tilde{h} \neq 0$). This conclusion is not trivial because the rotating field has no component in the direction of the induced magnetization. The value of this magnetization grows with decreasing temperature and its sign is determined by the direction of the magnetic field rotation, i.e., sgn $\mu_\infty=-\rho$. In particular, if $|\tilde{h}_{\text{eff}}| \ll 1$ then $t_{\text{rel}} = (T_0/2)\cosh^{-1}(2a\tilde{h}_{\text{eff}})$ and $\mu_\infty=\tanh(2a\tilde{h}_{\text{eff}})$. These results indicate that even a weak rotating field can drastically decrease the relaxation time and strongly magnetize the nanoparticle system if the temperature is low enough that $a|\tilde{h}_{\text{eff}}| \geq 1$. We note also that Eq. (5.4) overestimates the absolute value of the magnetization because the magnetic moment is less than m in the up state and larger than $-m$ in the down state.

B. Steady-state magnetization at high frequencies

In the case of a rapidly rotating field we are able to calculate the steady-state magnetization μ_∞ for an arbitrary anisotropy barrier. To this end, we introduce the stationary probability density $P_{\text{st}}=P_{\text{st}}(\theta,\psi)$ which, according to Eq. (2.7), satisfies the stationary (in the rotating frame) Fokker-Planck equation

$$\frac{\lambda}{2a}\left(\frac{\partial^2 P_{\text{st}}}{\partial\theta^2}+\frac{1}{\sin^2\theta}\frac{\partial^2 P_{\text{st}}}{\partial\psi^2}\right)-\frac{\partial}{\partial\theta}\left(\frac{\lambda}{2a}\cot\theta+u(\theta,\psi)\right)P_{\text{st}}$$
$$-\frac{\partial}{\partial\psi}[v(\theta,\psi)-\rho\Omega]P_{\text{st}}=0, \qquad (5.5)$$

being properly normalized, $\int_0^{2\pi}d\psi\int_0^\pi d\theta\, P_{\text{st}}=1$. Using the decompositions $P_{\text{st}}=\bar{P}_{\text{st}}(\theta)+P_1(\theta,\psi)$ ($\bar{P}_1=0$), $u(\theta,\psi)=\bar{u}(\theta)+u_1(\theta,\psi)$ ($\bar{u}_1=0$), and $v(\theta,\psi)=\bar{v}(\theta)+v_1(\theta,\psi)$ ($\bar{v}_1=0$), where the overbar denotes averaging over ψ, i.e., $\overline{(\cdot)}=(1/2\pi)\int_0^{2\pi}d\psi(\cdot)$, we obtain from Eq. (5.5) coupled equations for $\bar{P}_{\text{st}}$,

$$\frac{\lambda}{2a}\frac{d^2\bar{P}_{\text{st}}}{d\theta^2}-\frac{d}{d\theta}\left(\frac{\lambda}{2a}\cot\theta+\bar{u}\right)\bar{P}_{\text{st}}-\frac{d}{d\theta}\overline{u_1 P_1}=0, \quad (5.6)$$

and P_1

$$\frac{\lambda}{2a}\left(\frac{\partial^2 P_1}{\partial\theta^2}+\frac{1}{\sin^2\theta}\frac{\partial^2 P_1}{\partial\psi^2}\right)-\frac{\partial}{\partial\theta}\left(\frac{\lambda}{2a}\cot\theta+u(\theta,\psi)\right)P_1$$
$$+\rho\Omega\frac{\partial}{\partial\psi}P_1-\frac{\partial}{\partial\psi}v_1\bar{P}_{\text{st}}-\frac{\partial}{\partial\theta}u_1\bar{P}_{\text{st}}+\frac{d}{d\theta}\overline{u_1 P_1}$$
$$-\frac{\partial}{\partial\psi}v(\theta,\psi)P_1=0. \qquad (5.7)$$

Assuming that $P_1 \sim \Omega^{-1}$ as $\Omega \to \infty$, Eq. (5.7) reduces in the high-frequency limit to

$$\rho\Omega\frac{\partial}{\partial\psi}P_1 = \frac{\partial}{\partial\psi}v_1\bar{P}_{st} + \frac{\partial}{\partial\theta}u_1\bar{P}_{st}. \tag{5.8}$$

Since $v_1 = -\tilde{h}(\cos\theta\cos\psi + \lambda\sin\psi)/\sin\theta$ and $u_1 = \tilde{h}(\lambda\cos\theta\cos\psi - \sin\psi)$, the last equation has the solution

$$P_1 = -\rho\frac{\tilde{h}}{\Omega}(\cos\theta\cos\psi + \lambda\sin\psi)\frac{\bar{P}_{st}}{\sin\theta}$$

$$+ \rho\frac{\tilde{h}}{\Omega}\frac{\partial}{\partial\theta}(\lambda\cos\theta\sin\psi + \cos\psi)\bar{P}_{st}. \tag{5.9}$$

Evaluating the average

$$\overline{u_1 P_1} = \rho\frac{\lambda\tilde{h}^2}{\Omega}\sin\theta\bar{P}_{st}, \tag{5.10}$$

Eq. (5.6) becomes

$$\frac{\lambda}{2a}\frac{d^2\bar{P}_{st}}{d\theta^2} - \frac{d}{d\theta}\left(\frac{\lambda}{2a}\cot\theta - \lambda(\cos\theta + \tilde{h}_{eff})\sin\theta\right)\bar{P}_{st} = 0. \tag{5.11}$$

The normalized solution of this equation assumes the form

$$\bar{P}_{st}(\theta) = C\sin\theta\exp[-2a\tilde{W}_{eff}(\theta)], \tag{5.12}$$

where $\tilde{W}_{eff}(\theta) \equiv W_{eff}(\theta)/mH_a = (1/2)\sin^2\theta - \tilde{h}_{eff}\cos\theta$ is the dimensionless effective energy of the nanoparticle and

$$C = \sqrt{\frac{a}{\pi^3}}\frac{\exp[a(1+\tilde{h}_{eff}^2)]}{\mathrm{erfi}[\sqrt{a}(1+\tilde{h}_{eff})] + \mathrm{erfi}[\sqrt{a}(1-\tilde{h}_{eff})]} \tag{5.13}$$

is a normalizing constant derived from the condition $2\pi\int_0^\pi d\theta\,\bar{P}_{st}(\theta) = 1$. Here, $\mathrm{erfi}(z)$ stands for the imaginary error function defined as $\mathrm{erfi}(z) = (2/\sqrt{\pi})\int_0^z dx\,\exp(x^2)$.

Finally, using the definition of the steady-state magnetization $\mu_\infty = 2\pi\int_0^\pi d\theta\cos\theta\bar{P}_{st}(\theta)$, we obtain

$$\mu_\infty = \sqrt{\frac{1}{\pi a}}\frac{\exp[a(1+\tilde{h}_{eff})^2] - \exp[a(1-\tilde{h}_{eff})^2]}{\mathrm{erfi}[\sqrt{a}(1+\tilde{h}_{eff})] + \mathrm{erfi}[\sqrt{a}(1-\tilde{h}_{eff})]} - \tilde{h}_{eff}. \tag{5.14}$$

Since $\mathrm{erfi}(z) = 2(z + z^3/3 + \cdots)/\sqrt{\pi}$ if $z \ll 1$ and $\mathrm{erfi}(z) = \exp(z^2)(1/z + 1/2z^3 + \cdots)/\sqrt{\pi}$ if $z \gg 1$, in the case of a low anisotropy barrier ($a \ll 1$) this formula yields $\mu_\infty = 2a\tilde{h}_{eff}/3$, and in the case of a high anisotropy barrier ($a \gg 1$) and small effective field ($|\tilde{h}_{eff}| \ll 1$) it is reduced to the formula $\mu_\infty = \tanh(2a\tilde{h}_{eff})$, which coincides with that derived from the MFPT approach. As an illustration of the accuracy of (5.14) and the applicability of the MFPT approach for describing the magnetic relaxation in nanoparticle systems, we depict in Fig. 4 the theoretical and numerical results for the dependence of the induced magnetization μ_∞ on the anisotropy barrier height $a = mH_a/2k_BT$.
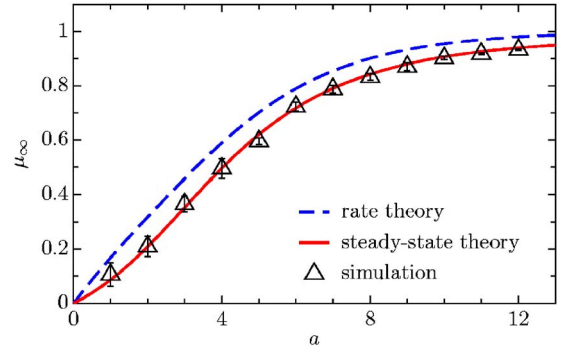

FIG. 4. (Color online) Dimensionless induced magnetization μ_∞ as a function of the anisotropy barrier height a for $\Omega = 10$, $\tilde{h} = 1$, $\rho = -1$, and $\lambda = 0.5$. The solid curve (red online) and the broken curve (blue online) represent the induced magnetization defined by the formulas (5.14) and (5.4) with (4.7), respectively. The triangular symbols indicate results obtained from the numerical simulation of Eqs. (2.10). As seen, the theoretical results that follow from the explicit solution of the Fokker-Planck equation are in excellent agreement with the numerical results. A small systematic shift of the induced magnetization derived within the rate theory arises from an overestimation of the absolute values of the average magnetic moment in the up and down states.

C. Numerical verification

As in the simulation of the MFPTs, described in the previous section, the Langevin equations (2.10) were used to compute the mean magnetization at high frequencies. However, the numerical simulation in this case differs from the case studied before in two important aspects. First, instead of an ensemble average over magnetic nanoparticles, a single, stochastic magnetic moment was averaged over time, thereby making use of ergodicity. Second, instead of using a reflecting and an absorbing boundary, here two reflecting boundaries were located at $\theta = 0.01\pi$ and 0.99π. For fixed parameter values $\Omega = 10$, $\tilde{h} = 1$, $\rho = -1$, $\lambda = 0.5$, four trajectories were simulated for each value of a. Each trajectory was initialized with $\theta = 0.05\pi$ and $\psi = \pi$. We introduced two circles as marks on the sphere at $\theta = 0.2\pi$ and 0.8π and defined a sign change of the magnetic moment as a crossing of the $\theta = 0.8\pi$ ($\theta = 0.2\pi$) mark, provided the magnetic moment had been in the $\theta \leqslant 0.2\pi$ ($\theta \geqslant 0.8\pi$) domain before. Each trajectory was run until 200 such sign changes had occurred. The projection of the magnetic moment on the easy axis was summed over all time steps and divided by the number of time steps at the end of the simulation. The convergence of the mean magnetic moment along these trajectories was monitored and found to have converged after 200 sign changes. From the four values for the mean magnetization, a mean value and a standard deviation were determined. Figure 4 depicts that the simulation and the analytic result of the steady-state theory at high frequencies, Eq. (5.14), are in very good agreement, indicating that the high-frequency limit is already obtained for $\Omega = 10$.

VI. CONCLUSIONS

We carried out a comprehensive study of the two-dimensional MFPT problem for the magnetic moment of a

nanoparticle driven by a magnetic field rapidly rotating in the plane perpendicular to the easy axis of magnetization. Our approach is based on Eqs. (3.7) and (3.8) for the MFPTs that we derived from the backward Fokker-Planck equation in the rotating frame. In the high-frequency limit, we solved these equations analytically and calculated the MFPTs for the nanoparticle magnetic moment in the up and down states. The main finding is that a rapidly rotating field influences the MFPTs due to the change of the potential barrier between these states, which occurs under the action of the static effective magnetic field applied along the easy axis of magnetization. We showed that the magnetic field rotating in the clockwise (counterclockwise) direction increases the MFPT for the magnetic moment in the up (down) state and decreases it for the magnetic moment in the down (up) state. Our theoretical predictions are in good agreement with the results obtained by numerical solution of the effective stochastic Landau-Lifshitz equations.

In addition, we applied the derived MFPTs to study the features of magnetic relaxation in nanoparticle systems caused by a rotating magnetic field. We established that in the case of a large anisotropy barrier this field always decreases the relaxation time and magnetizes the nanoparticle system. The magnetization grows as the temperature decreases and its direction is uniquely determined by the direc-

tion of field rotation. Solving the forward Fokker-Planck equation in the case of a rapidly rotating field, we calculated also the magnetization for an arbitrary anisotropy barrier. The theoretical results are in excellent agreement with the numerical ones and confirm the applicability of the MFPT approach for describing the magnetic relaxation in systems of high-anisotropy nanoparticles driven by a rapidly rotating magnetic field.

Due to the selective change of the noise-induced stability of a rapidly driven magnetic moment of a nanoparticle, as represented by the corresponding mean first-passage times, the results herein can be used for potential applications in magnetic recording technology. The relative stability of the magnetic moment in the up and down states can be suitably controlled either by changing the temperature T of the environment (thereby changing the anisotropy barrier height) or upon varying the strength of a rapidly rotating magnetic field.

ACKNOWLEDGMENTS

[1] P. Hänggi, P. Talkner, and M. Borkovec, Rev. Mod. Phys. **62**, 251 (1990).

[2] C. W. Gardiner, *Handbook of Stochastic Methods*, 2nd ed. (Springer-Verlag, Berlin, 1990).

[3] S. Redner, *A Guide to First-Passage Processes* (Cambridge University Press, Cambridge, U.K., 2001).

[4] L. S. Pontryagin, A. A. Andronov, and A. A. Vitt, Zh. Eksp. Teor. Fiz. **3**, 165 (1933).

[5] R. L. Stratonovich, *Topics in the Theory of Random Noise* (Gordon and Breach, New York, 1963), Vol. 1.

[6] N. S. Goel and N. Richter-Dyn, *Stochastic Models in Biology* (Academic Press, New York, 1975).

[7] G. H. Weiss, Adv. Chem. Phys. **13**, 1 (1966).

[8] P. Reimann and P. Hänggi, Appl. Phys. A: Mater. Sci. Process. **75**, 169 (2002); R. D. Astumian, Phys. Today **55**(11), 33 (2002); P. Hänggi, F. Marchesoni, and F. Nori, Ann. Phys. **14**, 51 (2005).

[9] Ratchets and Brownian Motors: Basics, Experiments and Applications, edited by H. Linke, special issue of Appl. Phys. A: Mater. Sci. Process. **75**, 167 (2002).

[10] L. Gammaitoni, P. Hänggi, P. Jung, and F. Marchesoni, Rev. Mod. Phys. **70**, 223 (1998).

[11] P. Hänggi, ChemPhysChem **3**, 285 (2002).

[12] D. Ryter, P. Talkner, and P. Hänggi, Phys. Lett. **93**, 447 (1983).

[13] P. Talkner and P. Hänggi, Phys. Rev. A **29**, 768 (1984).

[14] P. Talkner, New J. Phys. **1**, 4 (1999).

[15] J. Lehmann, P. Reimann, and P. Hänggi, Phys. Rev. Lett. **84**, 1639 (2000); Phys. Rev. E **62**, 6282 (2000); Phys. Status Solidi B **237**, 53 (2003).

[16] R. S. Maier and D. L. Stein, Phys. Rev. Lett. **86**, 3942 (2001).

[17] M. Schindler, P. Talkner, and P. Hänggi, Phys. Rev. Lett. **93**, 048102 (2004).

[18] P. Talkner and J. Łuczka, Phys. Rev. E **69**, 046109 (2004).

[19] M. Schindler, P. Talkner, and P. Hänggi, Physica A **351**, 40 (2005).

[20] S. I. Denisov, T. V. Lyutyy, P. Hänggi, and K. N. Trohidou, Phys. Rev. B **74**, 104406 (2006).

[21] S. I. Denisov, T. V. Lyutyy, and P. Hänggi, Phys. Rev. Lett. **97**, 227202 (2006).

[22] S. I. Denisov, K. Sakmann, P. Talkner, and P. Hänggi, Europhys. Lett. **76**, 1001 (2006).

[23] R. Kubo and N. Hashitsume, Suppl. Prog. Theor. Phys. **46**, 210 (1970).

[24] T. L. Gilbert, Phys. Rev. **100**, 1243 (1955).

[25] W. F. Brown, Jr., Phys. Rev. **130**, 1677 (1963).

[26] J. L. García-Palacios and F. J. Lázaro, Phys. Rev. B **58**, 14937 (1998).

[27] P. Hänggi, Helv. Phys. Acta **51**, 183 (1978).

[28] P. Hänggi and H. Thomas, Phys. Rep. **88**, 207 (1982).

[29] D. V. Berkov, IEEE Trans. Magn. **38**, 2489 (2002).

[30] D. V. Berkov and N. L. Gorn, J. Phys.: Condens. Matter **14**, L281 (2002).

[31] R. L. Stratonovich, SIAM J. Control **4**, 362 (1966).

[32] P. Hänggi and P. Riseborough, Am. J. Phys. **51**, 347 (1983).

[33] P. Hänggi and F. Marchesoni, Chaos **15**, 026101 (2005).

[34] M. Mangel, SIAM J. Appl. Math. **36**, 544 (1979); D. Ryter, Physica A **142**, 103 (1987); M. M. Klosek, B. J. Matkowsky, and Z. Schuss, Ber. Bunsenges. Phys. Chem. **95**, 331 (1991).

[35] P. Talkner, Chem. Phys. **180**, 199 (1994).

[36] G. Bertotti, C. Serpico, and I. D. Mayergoyz, Phys. Rev. Lett. **86**,

724 (2001).

[37] H. Risken, *The Fokker-Planck Equation*, 2nd ed. (Springer-Verlag, Berlin, 1989).

[38] S. I. Denisov and A. N. Yunda, Physica B **245**, 282 (1998).

[39] S. I. Denisov, T. V. Lyutyy, and K. N. Trohidou, Phys. Rev. B **67**,

014411 (2003).

[40] T. C. Gard, *Introduction to Stochastic Differential Equations*, Pure and Applied Mathematics Vol. 114 (Marcel Dekker, New York, 1988).